Sequential ctDNA whole-exome sequencing in advanced lung adenocarcinoma with initial durable tumor response on immune checkpoint inhibitor and late progression

Étienne Giroux Leprieur, Zofia Hélias-Rodzewicz, Paul Takam Kamga, Adrien Costantini, Catherine Julie, Alexandre Corjon, Coraline Dumenil, Jennifer Dumoulin, Violaine Giraud, Sylvie I. Labrune, et al.

Journal for ImmunoTherapy of Cancer

Sequential ctDNA whole-exome sequencing in advanced lung adenocarcinoma with initial durable tumor response on immune checkpoint inhibitor and late progression

Etienne Giroux Leprieur ,[1,2] Zofia Hélias-Rodzewicz,[1,3] Paul Takam Kamga,[1] Adrien Costantini,[1,2] Catherine Julie,[1,3] Alexandre Corjon,[1,3] Coraline Dumenil,[2] Jennifer Dumoulin,[2] Violaine Giraud,[2] Sylvie Labrune,[2] Simon Garinet,[4] Thierry Chinet,[1,2] Jean-François Emile[1,3]

To cite: Giroux Leprieur E, Hélias-Rodzewicz Z, Takam Kamga P, *et al*. Sequential ctDNA whole-exome sequencing in advanced lung adenocarcinoma with initial durable tumor response on immune checkpoint inhibitor and late progression. *Journal for ImmunoTherapy of Cancer* 2020;**8**:e000527. doi:10.1136/jitc-2020-000527

► Additional material is published online only. To view please visit the journal online (http://dx.doi.org/10.1136/jitc-2020-000527).

Accepted 13 April 2020

For numbered affiliations see end of article.

Correspondence to
Professor Etienne Giroux Leprieur;
etienne.giroux-leprieur@aphp.fr

ABSTRACT

Background Despite prolonged tumor response to immune checkpoint inhibitors (ICIs) for a subset of patients with advanced non-small cell lung cancer (NSCLC), a secondary resistance will occur for a majority of these patients. The understanding of late progression mechanisms with ICIs is important to improve future treatment strategies.

Methods We performed whole-exome sequencing (WES) on circulating tumor DNA and compared molecular profiles between the beginning of ICI treatment and tumor progression in patients with advanced NSCLC treated with ICIs and who had initial and prolonged tumor response with secondary progression, after at least 6 months of treatment.

Results We identified eight patients who experienced initial and durable tumor response, and secondary tumor progression after 6 months of treatment, with available paired blood samples (diagnosis and progression). All had lung adenocarcinoma, three had programmed-death ligand-1 expression ≥50% in immunohistochemistry and all presented low blood tumor mutational burden (bTMB). Seven patients received nivolumab in second-line or more, and one received pembrolizumab as first-line treatment. WES at progression showed clonal selection with molecular alterations of Wnt pathway-related genes, increase of copy number aberrations in cancer-related genes and loss of tumor-suppressor genes (such as *PTEN*) or of genes associated with immune response (such as *B2M*). No difference in term of bTMB was observed at progression.

Conclusions This is the first study describing putative molecular mechanisms associated with late progression under ICI in lung cancer. Studies on treatment strategies adapted to these mechanisms are needed.

INTRODUCTION

Prognosis of advanced non-small cell lung cancer (NSCLC) has greatly improved with the development of immune checkpoint inhibitors (ICIs).[1] Monoclonal antibodies targeting programmed-death-1 (PD-1) or programmed-death ligand-1 (PD-L1) are able to restore cytotoxic immune response. In advanced NSCLC, nivolumab, atezolizumab and pembrolizumab are currently approved in the second-line setting.[2–5] In the first-line setting, pembrolizumab is approved in case of high PD-L1 expression (≥50% in immunohistochemistry (IHC)),[6] or in combination with cytotoxic chemotherapy regardless of PD-L1 expression.[7 8] Atezolizumab is also approved in first-line treatment of metastatic non-squamous NSCLC in association with bevacizumab—carboplatin–paclitaxel or carboplatin–nab-paclitaxel.[9 10] Predictive biomarkers of ICIs efficacy have been widely studied. The levels of PD-L1 expression and tumor infiltration by immune cells, and high tumor mutational burden (TMB) correlate with survival when ICIs are given in monotherapy.[11] TMB is usually assessed on tumor tissue (tTMB) by whole exome sequencing (WES), even if large next-generation sequencing (NGS) panels can also be used.[12] Recent studies have shown that circulating tumor DNA (ctDNA) sequencing (by WES or large NGS panels) is feasible and could measure blood TMB (bTMB) efficiently, with good correlation with ICIs efficacy.[13] This strategy is very promising, as ctDNA reflects the different tumor clones, and blood is easily collected, whereas tTMB is feasible in only 50% of patients due to tissue availability.[14]

There are however little published data on resistance mechanisms with ICIs, especially considering late progression after initial and prolonged tumor response. We propose to

comparatively study WES performed on ctDNA at ICI initiation and at late progression. We compared bTMB, mutational profiles, copy number aberrations (CNAs) and microsatellite instability (MSI).

METHODS

Patients

All consecutive patients with advanced NSCLC treated with ICIs in our Department between June 2015 and December 2017 were screened. Patients who underwent tumor response (ie, complete or partial response) with ICI, lasting at least 6 months and with secondary tumor progression, were included in the study. All patients had CT-scan of thorax and abdomen and brain imaging every 3 (with pembrolizumab) or 4 (with nivolumab) cycles. Tumor response was assessed locally in multidisciplinary board, including a radiologist specialized in thoracic oncology, and reviewed at the time of WES analyzes according to RECIST 1.1. Best overall response rate (ORR), progression-free survival (PFS) and overall survival (OS) were collected, with a cut-off point on 11 June 2019. Demographic and histomolecular data were retrospectively collected.

PD-L1 immunohistochemistry

PDL1 IHC was performed using an automated method (Leica) and the E1L3N anti-PD-L1 antibody (Cell Signaling Technology) diluted to the 1/80th on 4 µm slides from the treatment-naïve diagnostic samples. The assay was performed using human amygdala as positive control, and IgG as isotype negative control. Proportion (percentage) of positive tumor cells (membranous staining) was recorded. A minimum of 100 tumor cells was needed for interpretation.

Blood and plasma collection

After signature of a consent form, blood samples were collected at diagnosis and every 2 months during ICI treatment. One 10 mL-EDTA (Ethylenediaminetetraacetic acid) tube was collected and whole blood samples were conserved at −80°C for constitutive DNA analyzes. Two additional 10 mL-EDTA tubes of peripheral blood were taken, and plasma was isolated within 1 hour after centrifugation and immediately conserved at −80°C.

DNA extraction

ctDNA from plasma samples was extracted using AS1480 Maxwell RSC ccf DNA Plasma Kit (Promega, USA), according to manufacturer's instructions. DNA from whole blood samples (used for constitutive DNA) was extracted using AS1010 Maxwell 16 Blood DNA Purification Kit (Promega, USA), according to manufacturer's instructions. DNA concentrations were calculated using Multiscan GO reader, V.1.01.10 (ThermoFisher Scientific, France).

Targeted exome sequencing

WES was performed on samples taken at the beginning of ICI treatment and at the time of late progression. Library preparation, exome capture, sequencing and data analysis have been done by IntegraGen SA (France). Genomic DNA was captured using Twist Human Core Exome Enrichment System (Twist Bioscience)+IntegraGen Custom.[15] Sequence capture, enrichment and elution were performed according to manufacturer's instruction and protocols (Twist Bioscience) without modification except for library preparation performed with NEBNext Ultra II kit (New England Biolabs). For library preparation 150 ng of each genomic DNA were fragmented by sonication and purified to yield fragments of 150–200 bp. Paired-end adaptor oligonucleotides from the NEB kit were ligated on repaired, a-tailed fragments then purified and enriched by 7 PCR cycles. Five hundred ng of these purified Libraries were then hybridized to the Twist oligo probe capture library for 16 hours in a singleplex reaction. After hybridization, washing and elution, the eluted fraction was PCR amplified with eight cycles, purified and quantified by QPCR to obtain sufficient DNA template for downstream applications. Each eluted-enriched DNA sample was then sequenced on an Illumina NovaSeq as Paired-end 100 reads. Image analysis and base calling was performed using Illumina Real Time Analysis with default parameters. We aimed a tumorous exome depth of x270 and constitutive exome depth of x65.

Bioinformatics

Exome analysis

Sequence reads were mapped to the Human genome build (hg38) by using the Burrows-Wheeler Aligner tool. The duplicate reads (eg, paired-end reads in which the insert DNA molecules have identical start and end locations in the Human genome) were removed. Variant calling for the identification of single nucleotide variations (SNVs) and small insertions/deletions (up to 20 bp), was performed via the Broad Institute's GATK Haplotype Caller GVCF tool (GATK3.8.1) for constitutional DNA and via the Broad Institute's MuTect tool (2.0) for somatic DNA. For oncology analyzes, a Fisher's exact test was applied after MuTect2 variant calling to improve filtering of variants with strand bias. The panel of normal (PON) was a type of resource which used in somatic variant analysis when no normal is available. To create this PON, we used constitutional sample captured and sequenced at Integragen and in addition, the PON of Broad Institute. An in-house postprocessing to filter out candidate somatic mutations that were more consistent with artifacts or germline mutations was applied. Only the somatic mutations considered as PASS or t_lod_fstar were retained, and a somatic score of at least 1 was added with analysis without PON. The somatic score was calculated for each mutation ranging from 1 to 30, a score of 30 translating the highest confidence index. This score took into account the frequency and counts of mutated allele in both samples. Finally, the mutations with a score below 20 and a variant allelic frequency (VAF) of tumor <0.02 were removed. We also ran VarScan2 on somatic variants indicated as

clustered_events by Mutect2, and checked if any high confidence variants were also called (but subsequently filtered) by MuTect2.

Five bioinformatics algorithms for pathogenicity were available to predict the functional, molecular and phenotypic consequences of coding and non-coding single nucleotide polymorphisms (SNPs). This included DANN, FATHMM, MutationTaster, SIFT and Polyphen. The clinical and pathological significance from the ClinVar database was added.

Bioconductor DNACopy package was used to investigate genomic CNAs, by comparing the normal DNA exome data to a reference sample pool. It implements the circular binary segmentation algorithm to segment DNA copy number data.

Tumor mutational burden

TMB was calculated by dividing the number of somatic mutations by the number of bases having a depth greater than 10. The somatic mutations used for TMB were filtered as follows: Somatic score >3, FILTER=PASS, mutated allele frequency in tumor tissue ≥5%, mutated allele count in tumor tissue ≥3, mutated allele frequency in constitutional tissue <4%, IntegraGen het freq≤1%, IntegraGen heterozygous frequency ≤1%, IntegraGen homozygous frequency ≤1% and EVS and 100G and Exac variant frequency ≤0.5% and consequences on protein: Stop, Start, Missense, Splice for the SNPs and Inframe, Frameshift for the indels.

Microsatellite analysis

The MSI sensor software with default filters was used to detect variants in microsatellite regions and annotate them as germline or somatic. The MSI threshold was 3.5% (11% in the case of PON analysis).

NGS analyses

Routine molecular screening was performed at diagnosis for all patients on tumor biopsies. DNAs were extracted on a Maxwell 16 Forensic Instrument (Promega, France) using Maxwell 16 FFPE Plus LEV DNA Purification Kit (Promega, France) for FFPE samples. Quantification was done by Qubit dsDNA BR Assay Kit (Thermo Fisher Scientific, France). *Colon and Lung Cancer Panel V2* libraries were prepared using the Ion Ampliseq library preparation kit v2 from 30 ng of tumor DNA. Libraries were normalized (Ion Library Equalizer Kit), pooled, processed on a Ion Chef System for template preparation and chip loading (Ion PI Hi-Q Chef Kit, Ion PI Chip Kit v3, Thermo Fisher Scientific), and sequenced on a Ion Proton System.

Survival analyses

PFS was calculated from the beginning of ICI until progression or death. OS was calculated from the beginning of ICI until death. Post-ICI OS was calculated from the last cycle of ICI until death. PFS, OS and post-ICI OS were calculated with Xlstat 2019.1.2 (Addinsoft, France).

RESULTS

Patients

Between June 2015 and December 2017, 79 consecutive patients with advanced NSCLC were treated by ICIs in our department (nivolumab in second line or more, n=73; pembrolizumab in first line, n=6). We identified 10 patients (12.7%) who experienced initial and durable (more than 6 months) tumor response (all with partial response), and secondary tumor progression after 6 months of treatment. Eight patients had paired blood samples (diagnosis and progression) available for analyzes. Main characteristics of the patients are reported in table 1. Median age was 70.2 years (range 43.5–84.8), five patients (63.0%) were male, and all had lung adenocarcinoma. Seven patients received nivolumab in second-line or more, and one received pembrolizumab as first-line treatment because of a high PD-L1 (50%) expression. Of the seven patients treated with nivolumab, best tumor response with previous chemotherapy line was partial response (n=1; 14.3%), stability (n=4; 57.1%) and tumor progression (n=2; 28.6%). Routine molecular screening at diagnosis showed a *KRAS* mutation within the tumors of five patients (62.5%). One patient (12.5%) had a tumor with high-level *Met* amplification (confirmed by fluorescence in situ hybridization). Three patients presented a *BRAF* mutation (G464V, n=2; G469V, n=1), alone (n=1) or associated with a *KRAS* mutation (n=2). Two patients (25.0%) did not have alteration of *KRAS*, *BRAF*, *EGFR*, *HER2* nor *MET* at diagnosis. Best tumor response with ICIs was partial response for all patients, all of which occurred at the first tumor evaluation. Clinical outcomes with ICI are presented in table 2. Median number of ICI cycles administered was 22 (range 12–42). Median PFS with ICIs was 12.1 months (IQR 9.0–14.6) (online supplementary figure 1A). Median OS with ICIs was not reached (NR) (IQR 23.5 – NR) (online supplementary figure 1B). Seven patients (87.5%) received a new systemic treatment after progression under ICIs. Median post-ICIs OS was NR (IQR 11.5–NR) (online supplementary figure 1C). At the time of progression with ICI, the majority of the patients experienced an extrathoracic progression (n=5; 62.5%). One patient had tumor progression restricted to the central nervous system (CNS) with appearance of brain metastases and carcinomatous meningitis.

WES at ICI initiation

At ICI initiation, ctDNA was detected in all eight plasma samples, with a median plasma DNA concentration of 3.3 ng/µL (range 2.0–15.7). Mean tumorous exome depth was x233 (range 195–315). WES analyzes did not show any *KRAS* mutation in any samples. Absence of *KRAS* mutation for patients #1, #2, #4 and #6 was confirmed using an NGS panel on these plasma, whose analytical sensitivity is around 0.5%.[16] Two samples (patients #3 and #8) harbored a *TP53* mutation (VAF of 8.3% and 6.8%), and one (patient #8) had a *KEAP1* mutation (VAF of 9.0%). Summary of molecular profile is presented in table 3. No gene amplification was observed.

Table 1 Main characteristics of the patients with initial tumor response and late progression on ICI

Patient	Gender	Tobacco use	Age	Histology	PD-L1 expression (%)	Molecular addiction at diagnosis	TNM stage	Metastatic sites at ICI initiation	No of chemotherapy line before ICI	Best response to previous treatment
#1	M	FS	77.0	AK	0	KRAS mutation	4	L	2	PD
#2	F	FS	65.5	AK	NA	KRAS mutation +G464V BRAF mutation	4	B, Li, A	1	SD
#3	M	FS	69.1	AK	80	G464V BRAF	4	Me, CL	1	PD
#4	M	S	65.1	AK	25	KRAS mutation	4	Me, P, A	3	SD
#5	F	S	73.6	AK	5	KRAS mutation +G469V BRAF mutation	4	Me, L, P, B, CNS	1	SD
#6	M	S	43.5	AK	NA	KRAS mutation	4	L, P	1	PR
#7	M	FS	84.8	AK	50	MET amplification	3	Me	0	–
#8	F	S	71.3	AK	50	None	4	Me, L, CNS	4	SD

A, adrenal; AK, adenocarcinoma; B, bone; CL, cervical lymphadenopathies; CNS, central nervous system; F, female; FS, former smoker; ICI, immune checkpoint inhibitor; L, lung; Li, liver; M, male; Me, mediastinum; NA, not available; P, pleura; PD, progressive disease; PD-L1, programmed-death ligand-1; PR, partial response; S, smoker; SD, stable disease.

At ICI initiation, the eight samples presented a low bTMB, with a median of 0.04 mutations per Mb (range 0.0–8.2). Median number of CNAs was 170.0 (range 116.0–347.0), almost exclusively loss of heterozygosity (LOH). Concerning cancer-related genes, number of CNAs was 28.5 (range 15.0–79.0).

WES at progression

At the time of late progression, ctDNA was detected in all eight plasma samples at the time of late progression, with a median plasma DNA concentration of 3.1 ng/µL (range 2.6–4.4). Mean tumorous exome depth was x233 (range 147–321). WES analyzes did not show any *Kras* mutation in any samples. However, we found both atypical *Braf* mutations (G464V with VAF of 10.6%, and G469V with VAF of 3.0%, respectively) that were present at diagnosis for patients #2 and #5. Interestingly, we found in patient #2 the emergence of 2 somatic mutations in Wnt pathway related-genes: a SNV *LRP1B* mutation (VAF 11.5%, splice-acceptor sequence) and a S213F *DVL1* mutation (VAF 4.1%, inducing a missense on the protein sequence). Another sample (patient #5) presented a P192H *RET* mutation (VAF 4.2%) inducing a missense on the protein sequence. A summary of the mutational profile of the eight samples is presented in table 3. No gene amplification was observed.

For patient #6 who presented a progression located exclusively in the CNS with brain metastases and carcinomatous meningitis (resulting in paraplegia and sphincter disorders), we performed a NGS analysis (Colon-Lung panel) on spinal fluid. We found a different tumor clone within the spinal fluid, with absence of *KRAS* mutation (detected in diagnostic sample), the presence of an exon 18 G719A activating *EGFR* mutation (VAF 4.0%), a *PTEN* mutation (VAF 2.5%) and a *TP53* mutation (VAF 2.0%). Comparison of polymorphisms between this sample and the sample at the time of diagnosis was concordant and confirmed they corresponded to the same patient. Patient #6 received therefore subsequent treatment after ICI with osimertinib, considering that thoracic disease was controlled at this time, resulting in a rapid clinical efficacy (spectacular improvement of neurologic symptoms) and stabilization of lesions on brain and spinal MRI at 2 months. Unfortunately, the patient experienced further CNS tumor progression 4 months after the beginning of osimertinib. New NGS analysis in spinal fluid at the time of progression with osimertinib showed the persistence of the exon 18 *EGFR, PTEN and TP53* mutations, the absence of *KRAS* mutation but the apparition of gene amplifications (*EGFR, DDR2 and AKT1*) that may explain the tumor progression.

The eight samples at the time of progression with ICI still had a low bTMB, with a median of 0.05 mutation per Mb (range 0.0–1.81). MSI status was negative for all tumors (median 0.2%; range 0.0–0.4).

Median number of CNAs was 183.0 (range 127.0–228.0), almost exclusively LOH, without numerical statistical difference compared with the beginning of ICI treatment.

Table 2 Type of ICI and clinical outcome at progression

Patient	ICI	No of ICI cycles	Site of progression with ICI	Systemic treatment after ICI progression
#1	Nivo	16	Me, P, L	Yes
#2	Nivo	18	L, Li	Yes
#3	Nivo	20	L	Yes
#4	Nivo	28	A	Yes
#5	Nivo	24	L, B	Yes
#6	Nivo	42	CNS	Yes
#7	Pembro	12	L	Yes
#8	Nivo	32	L, CNS	No

A, adrenal; B, bone; CL, cervical lymphadenopathies; CNS, central nervous system; ICI, immune checkpoint inhibitor; L, lung; Li, liver; Me, mediastinum; Nivo, nivolumab; P, pleura; Pembro, pembrolizumab.

However, looking at cancer-related genes, a majority of samples (n=5, 62.5%) at ICI progression showed a dramatic increase of CNAs (mean relative increase of +86% of cancer-related CNAs), with two patients (#7 and #8) with more than +130% relative increase of CNAs, whereas other patients (n=3, 37.5%) had moderate decrease of CNAs (mean relative decrease of −45% of cancer-related CNAs), compared with the beginning of ICI. All of the cancer-related CNAs concerned LOH. Interestingly, we found new loss of gene expressions concerning Wnt-related genes (*LRP5*, patient #6; *SETD6*, patient #8), gene associated with antigen presentation (*B2M*, patient #4), gene associated with recognition of tumor damage associated molecular patterns (*TLR8*, patient #4), tumor necrosis factor (TNF)-induced inflammation (*GADD45B*, patients #1, #3 and #8; *TNFRSF17*, patient #8), and LOH of immune checkpoint PD-L2 (*PDCD1LG2*, patient #8).

A summary of comparative molecular profiles is presented in table 3 and figure 1.

DISCUSSION

This study is the first to report comparative WES data on ctDNA in advanced NSCLC patients treated with ICIs, comparing molecular profile between treatment initiation and disease progression. Moreover, this is also the first study to specifically address the putative underlying molecular mechanisms of late progression after prolonged response with ICI in these patients. In literature, several resistance mechanisms to ICI have been described, but mainly in pre-clinical studies, or in other solid tumors, as melanoma. These mechanisms concern loss of antigen presentation (loss of type-I Major Histocompatibility Complex, LOH/mutation of *B2M*), mutations on genes involved in Interferon-gamma pathway (*JAK* mutations), and activation of specific pathways (Wnt pathway, PI3K-AKT-STAT3 pathway associated with loss of *PTEN*).[17]

We were able to show that late progression was associated with the emergence of new tumor clones. It was especially illustrated by the data from patient #6 who experienced CNS progression with nivolumab, and the description of an exon 18 *EGFR* mutation in spinal fluid whereas the initial tumor harbored a *KRAS* mutation. In some cases, we also showed the acquisition of new somatic mutations. In patient #5, WES at the time of progression showed a new *RET* mutation. RET is a tyrosine kinase receptor, with a pro-oncogenic role. *RET* mutations have been described in several solid tumors.[18] *RET* fusions occurred in around 1% of advanced NSCLC, and are also associated with resistance to Epidermal Growth Factor Receptor (EGFR) tyrosine kinase inhibitors (TKIs).[19] In patients #2, we described the emergence of 2 somatic mutation associated with Wnt pathway (*LRP1B* and *DVL1*). *DVL1* codes for a cytoplasmic protein (Disheveled) that is phosphorylated in case of beta-catenin-Wnt pathway activation, recruiting axin and activating B-catenin.[20] LRP proteins are membranous proteins, associated with Frizzled receptors, binding with Wnt proteins. LRP1B down-regulates the canonical Wnt signaling pathway, and *LRP1B* inactivation (by mutation or LOH) has been associated with resistance to chemotherapy and increased tumor growth and invasive capacity.[21 22] Interestingly, we also showed a LOH of another LRP gene (*LRP5*) in patient #6, and of *SETD6* gene. SETD6 is a methyltransferase protein (inducing notably methylation of NFKB and PAK4), is associated with Wnt pathway, and its inhibition induces tumor cell motility.[23] Taken together, these data suggests a potential role of Wnt pathway in late progression with ICI. Wnt pathway has already been described as associated with ICI resistance and low inflammation levels, but mainly in early primitive resistance in other solid tumors such as melanoma.[24] This study is the first to suggest its role in secondary resistance in advanced NSCLC.

We were able to show an important increase of CNAs related to cancer associated genes in five samples at the time of progression. CNAs are known to be associated with ICI efficacy. In three independent cohorts of cancer patients (NSCLC and melanoma) treated with ICI, a low number of CNAs was associated with better outcome.[25] A high number of CNAs seems to be correlated with low tumor inflammation, and therefore poor response to ICI.[26] Preliminary data have also shown that loss of *PTEN*, detected in three

Table 3 Comparative molecular profile on ctDNA between ICI initiation and late progression

patient	somatic mutations at ICI initiation (%VAF)	somatic mutations at ICI progression (%VAF)	new LOH of specific cancer-related genes at ICI progression
#1	HOXA13 (7.6) INSR (19.5)	APAF1 (2.0) ATM (2.0) HOXA13 (13.1) FOXL2 (5.2)	BAP1, CCND3, GADD45B, HLA-A, HLA-B, PIK3R3, PTEN, SMARCD1, XPC
#2	BLK (4.4) FOXL2 (7.1)	ARID3C (3.7) MAX (10.9) G464V BRAF (10.6) NUP93 (4.0) DVL1 (4.1) PAG1 (7.7) LRP1B (11.5) SHTN1 (4.7) MAML2 (3.2)	HSPB1, STK19
#3	ATR (6.9) NF1 (6.9) G464V BRAF (7.4) PHOX2B (8.5) CDKN2 (4.0) PIM1 (8.4) HOXA13 (6.6) TP53 (8.3)	DNMT3B (5.2)	B2M, DNAJB1, GADD45B, LTB, TGFBR2
#4	AR (12.0) FAT1 (3.0)	FAT1 (3.5)	RASA1, SH3GL1, SMARCE1, TLR8
#5	HOXA13 (12.5)	G469V BRAF (3.0) KMT2D (4.9) BLK (3.8) MUC1 (9.0) CLIP1 (4.9) RET (4.2) FOXL2 (7.9) ZFHX3 (5.2) HOXA13 (17.4)	CCND3, DEK, DNAJB1, LRP5, MAP2K4, MAPK3
#6	CDKN2 (1.9) FOXL2 (5.0) HOXA13 (9.4)	G719A EGFR (4.0)* PTEN (2.5)* TP53 (2.0)*	DNAJB1, NFKB2, SMARCE1
#7	FOXL2 (7.3) PHOX2B (5.8)	ARID1B (6.4) FOXL2 (3.5)	CCND3, CXCR3, FBXO31, HSPB1, PTEN, RB1, SETD6, XPC
#8	ARID1A (18.5) KEAP1 (9.0) ATXN2 (9.1) LRP1B (5.5) BCL12B (5.2) MNX1 (11.3) BCR (25.6) MST1 (8.8) CPS1 (10.7) MYBL1 (9.6) DOT1L (11.5) NCOA3 (4.5) EP300 (17.2) NUTM2B (21.7) EPHA5 (16.6) PAX7 (6.0) FAF1 (10.5) POLD1 (12.1) FGFR3 (6.8) RELN (13.9) FOXL2 (5.6) SEC31A (5.8) GABRA6 (13.9) TMEM127 (15.9) INSR (7.3) TP53 (6.8)	FOXL2 (5.3)	GADD45B, NFKBIE, NOTCH4, PCD1LG2, PTEN, SMARCD2, TNFRSF17

Underlined genes correspond to new somatic mutations compared with ICI initiation.
*Molecular pattern determined by NGS on spinal fluid.
ctDNA, circulating tumor DNA; ICI, immune checkpoint inhibitor; LOH, loss of heterozygosity; NGS, next-generation sequencing; VAF, variant allelic frequency.

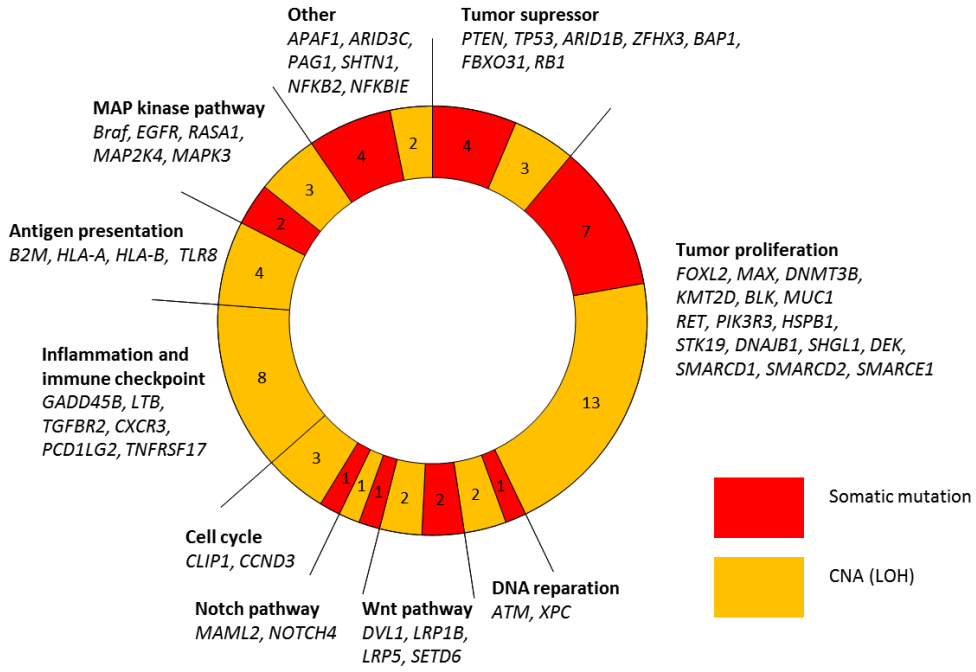

Figure 1 Graphical view of acquired gene alterations (somatic mutations, CNAs) at late progression with ICI. Numbers are the number of time each gene alteration was detected by sequencing. CNA, copy number aberration; ICI, immune checkpoint inhibitor; LOH, loss of heterozygosity.

samples at the time of progression in our study (with also a *PTEN* mutation detected in patient #6), was associated with ICI resistance in murine models and in a patient with early progression to ICI.[27 28] Moreover, in our work, one patient presented with a loss of *B2M* coding for Beta-2 microglobulin protein. *B2M* mutation has already been described as associated with progression with ICI, especially in melanoma.[29] Loss of *B2M* has also been described as associated with progression with ICIs in a small cohort of melanoma patients[30] and in one patient with NSCLC.[31] At last, several aberrations on other genes, related with inflammation and neoantigene recognition by immune cells, have been detected at the time of progression in our work, suggesting adaptive molecular mechanism to escape immune response. Importantly, we described the loss of expression of *PDCD1LG2* gene, coding for PD-L2, in a patient with late progression with nivolumab. Nivolumab is an anti-PD-1 antibody, targeting both immune checkpoints PD-L1 and PD-L2. Loss of PD-L2 expression could therefore induce resistance to nivolumab.

We did not find any modification of bTMB at late progression. All of the tumors presented low bTMB at the beginning of ICI, and kept low levels at progression. Gandara *et al* recently showed the feasibility and potential interest of bTMB in patients treated with ICI monotherapy.[13] Our results suggest that bTMB is not a biomarker associated with late progression. However, the small number of patients limits the interpretation of this result.

Our work has several limitations. First, for several patients, we did not find the same molecular pattern between diagnosis (NGS panel on tumor biopsies) and the beginning of ICI (WES on ctDNA). We confirmed the absence of *Kras* mutation at the beginning of ICI with a highly sensitive technique (NGS panel). The first explanation is that, for all patients except one, ICI was administered in second-line or more. A clonal selection before the beginning of ICI is therefore possible. The increased of genomic instability (attested by LOH) might be responsible for emerging of new clones with simultaneous loss of oncogenic addiction (attested by loss of *KRAS* mutation) and loss of the targets of the immune response. Moreover, we know that molecular analyzes on ctDNA have slightly lower sensitivity compared with analyzes performed on FFPE tissues. It is particularly true for gene amplifications, and this could explain the absence of *MET* amplification detected on WES for patient #7. To be noted, other mutations as non-V600 *BRAF* mutations present for two patients at diagnosis were found on WES. Concerning other frequent mutations observed on plasma at ICI initiation and not at the diagnosis, as *TP53* mutations, these mutations were not searched routinely for our patients at the time of diagnosis. Another limitation is the absence of *in vitro* analyzes to confirm the impact of molecular abnormalities at progression on ICI resistance. This is a pilot study, and these preliminary results need to be further explored. However, several molecular pattern found at progression have already been correlated with ICI resistance / progression in other pre-clinical studies. This study has also some strengths. It is the first study dedicated to molecular pattern at late progression after initial response with ICI in NSCLC. We were also able to perform WES on ctDNA for all eight patients both at the initiation of ICI and at the time of progression, allowing comparative study.

In conclusion, the description and comprehension of biological mechanisms associated with late progression on ICIs, especially after prolonged tumor response, is a critical

step in order to improve future treatment strategies, and target specific molecular pathways. Clonal selection, Wnt pathway and loss of genes associated with immune response seem to be associated with late progression under ICI monotherapy. Further studies, in larger populations and with ICI combination treatments are needed.

Author affiliations
[1]Université Paris-Saclay, UVSQ, EA 4340 BECCOH, Boulogne-Billancourt, France
[2]Department of Respiratory DIseases and Thoracic Oncology, APHP - Hopital Ambroise Pare, Boulogne-Billancourt, France
[3]Department of Pathology, APHP - Hopital Ambroise Pare, Boulogne-Billancourt, France
[4]Department of Molecular Biology, APHP - Hopital Europeen Georges Pompidou, Paris, France

Contributors EGL: conception of the project, data analyses, data collection and analyses, statistical analyses, writing of the manuscript, revision of the manuscript. ZH-R and SG: data analyses, revision of the manuscript. PTK, AdC, AIC, CJ, CD, JD, VG, SL, SG, J-FE and TC: revision of the manuscript.

Funding The authors have not declared a specific grant for this research from any funding agency in the public, commercial or not-for-profit sectors.

Competing interests J-FE: Bristol-Myers-Squibb (advisory board). EGL: Bristol-Myers-Squibb (honoraria, advisory board, research funding)

Patient consent for publication Not required.

Ethics approval Whole blood and plasma were conserved at Hospital Ambroise Paré Biological Resources Center (AFNOR NF-96900 certification). The protocol was approved by the Institutional Review Board CPP IDF n°8.

Provenance and peer review Not commissioned; externally peer reviewed.

Data availability statement Data are available on reasonable request. The datasets used and/or analyzed during the current study are available from the corresponding author on reasonable request.

ORCID iD
Etienne Giroux Leprieur http://orcid.org/0000-0001-8441-1701

REFERENCES

1 Giroux Leprieur E, Dumenil C, Julie C, *et al*. Immunotherapy revolutionises non-small-cell lung cancer therapy: results, perspectives and new challenges. *Eur J Cancer* 2017;78:16–23.
2 Borghaei H, Paz-Ares L, Horn L, *et al*. Nivolumab versus docetaxel in advanced Nonsquamous non-small-cell lung cancer. *N Engl J Med* 2015;373:1627–39.
3 Brahmer J, Reckamp KL, Baas P, *et al*. Nivolumab versus docetaxel in advanced squamous-cell non-small-cell lung cancer. *N Engl J Med* 2015;373:123–35.
4 Rittmeyer A, Barlesi F, Waterkamp D, *et al*. Atezolizumab versus docetaxel in patients with previously treated non-small-cell lung cancer (oak): a phase 3, open-label, multicentre randomised controlled trial. *Lancet* 2017;389:255–65.
5 Herbst RS, Baas P, Kim D-W, *et al*. Pembrolizumab versus docetaxel for previously treated, PD-L1-positive, advanced non-small-cell lung cancer (KEYNOTE-010): a randomised controlled trial. *Lancet* 2016;387:1540–50.
6 Reck M, Rodríguez-Abreu D, Robinson AG, *et al*. Pembrolizumab versus chemotherapy for PD-L1-positive non-small-cell lung cancer. *N Engl J Med* 2016;375:1823–33.
7 Gandhi L, Rodríguez-Abreu D, Gadgeel S, *et al*. Pembrolizumab plus chemotherapy in metastatic non-small-cell lung cancer. *N Engl J Med* 2018;378:2078–92.
8 Paz-Ares L, Luft A, Vicente D, *et al*. Pembrolizumab plus chemotherapy for squamous non-small-cell lung cancer. *N Engl J Med* 2018;379:2040–51.
9 Socinski MA, Jotte RM, Cappuzzo F, *et al*. Atezolizumab for first-line treatment of metastatic Nonsquamous NSCLC. *N Engl J Med* 2018;378:2288–301.
10 West H, McCleod M, Hussein M, *et al*. Atezolizumab in combination with carboplatin plus nab-paclitaxel chemotherapy compared with chemotherapy alone as first-line treatment for metastatic non-squamous non-small-cell lung cancer (IMpower130): a multicentre, randomised, open-label, phase 3 trial. *Lancet Oncol* 2019;20:924–37.
11 Prelaj A, Tay R, Ferrara R, *et al*. Predictive biomarkers of response for immune checkpoint inhibitors in non-small-cell lung cancer. *Eur J Cancer* 2019;106:144–59.
12 Chan TA, Yarchoan M, Jaffee E, *et al*. Development of tumor mutation burden as an immunotherapy biomarker: utility for the oncology clinic. *Ann Oncol* 2019;30:44–56.
13 Gandara DR, Paul SM, Kowanetz M, *et al*. Blood-Based tumor mutational burden as a predictor of clinical benefit in non-small-cell lung cancer patients treated with atezolizumab. *Nat Med* 2018;24:1441–8.
14 Hellmann MD, Ciuleanu T-E, Pluzanski A, *et al*. Nivolumab plus ipilimumab in lung cancer with a high tumor mutational burden. *N Engl J Med* 2018;378:2093–104.
15 Gnirke A, Melnikov A, Maguire J, *et al*. Solution hybrid selection with ultra-long oligonucleotides for massively parallel targeted sequencing. *Nat Biotechnol* 2009;27:182–9.
16 Didelot A, Le Corre D, Luscan A, *et al*. Competitive allele specific TaqMan PCR for KRAS, BRAF and EGFR mutation detection in clinical formalin fixed paraffin embedded samples. *Exp Mol Pathol* 2012;92:275–80.
17 Kalbasi A, Ribas A. Tumour-Intrinsic resistance to immune checkpoint blockade. *Nat Rev Immunol* 2020;20:25–39.
18 Drilon A, Hu ZI, Lai GGY, *et al*. Targeting RET-driven cancers: lessons from evolving preclinical and clinical landscapes. *Nat Rev Clin Oncol* 2018;15:151–67.
19 Piotrowska Z, Isozaki H, Lennerz JK, *et al*. Landscape of Acquired Resistance to Osimertinib in *EGFR*-Mutant NSCLC and Clinical Validation of Combined *EGFR* and *RET* Inhibition with Osimertinib and BLU-667 for Acquired *RET* Fusion. *Cancer Discov* 2018;8:1529–39.
20 Duchartre Y, Kim Y-M, Kahn M. The Wnt signaling pathway in cancer. *Crit Rev Oncol Hematol* 2016;99:141–9.
21 Zilberberg A, Yaniv A, Gazit A. The low density lipoprotein receptor-1, LRP1, interacts with the human frizzled-1 (HFz1) and down-regulates the canonical Wnt signaling pathway. *J Biol Chem* 2004;279:17535–42.
22 Prazeres H, Torres J, Rodrigues F, *et al*. Chromosomal, epigenetic and microRNA-mediated inactivation of LRP1B, a modulator of the extracellular environment of thyroid cancer cells. *Oncogene* 2011;30:1302–17.
23 Vershinin Z, Feldman M, Chen A, *et al*. Pak4 methylation by SETD6 promotes the activation of the Wnt/β-catenin pathway. *J Biol Chem* 2016;291:6786–95.
24 Spranger S, Bao R, Gajewski TF. Melanoma-intrinsic β-catenin signalling prevents anti-tumour immunity. *Nature* 2015;523:231–5.
25 Liu L, Bai X, Wang J, *et al*. Combination of TMB and CNA Stratifies prognostic and predictive responses to immunotherapy across metastatic cancer. *Clin Cancer Res* 2019;25:7413–23.
26 Roh W, Chen P-L, Reuben A, *et al*. Integrated molecular analysis of tumor biopsies on sequential CTLA-4 and PD-1 blockade reveals markers of response and resistance. *Sci Transl Med* 2017;9:eaah3560.
27 Peng W, Chen JQ, Liu C, *et al*. Loss of PTEN promotes resistance to T cell-mediated immunotherapy. *Cancer Discov* 2016;6:202–16.
28 George S, Miao D, Demetri GD, *et al*. Loss of PTEN is associated with resistance to anti-PD-1 checkpoint blockade therapy in metastatic uterine leiomyosarcoma. *Immunity* 2017;46:197–204.
29 Zaretsky JM, Garcia-Diaz A, Shin DS, *et al*. Mutations associated with acquired resistance to PD-1 blockade in melanoma. *N Engl J Med* 2016;375:819–29.
30 Sade-Feldman M, Jiao YJ, Chen JH, *et al*. Resistance to checkpoint blockade therapy through inactivation of antigen presentation. *Nat Commun* 2017;8:1136.
31 Gettinger S, Choi J, Hastings K, *et al*. Impaired HLA class I antigen processing and presentation as a mechanism of acquired resistance to immune checkpoint inhibitors in lung cancer. *Cancer Discov* 2017;7:1420–35.